PRAMANA
— journal of
physics

Vol. 81, No. 2
August 2013
pp. 295–308

Temporal dynamics of high repetition rate pulsed single longitudinal mode dye laser

G SRIDHAR*, V S RAWAT, S SINGH and L M GANTAYET
Laser & Plasma Technology Division, Bhabha Atomic Research Centre, Mumbai 400 085, India
*Corresponding author. E-mail: gsridhar@barc.gov.in

MS received 12 April 2012; revised 30 January 2013; accepted 30 April 2013

Abstract. Theoretical and experimental studies of temporal dynamics of grazing incidence grating (GIG) cavity, single-mode dye laser pumped by high repetition rate copper vapour laser (CVL) are presented. Spectral chirp of the dye laser as they evolve in the cavity due to transient phase dynamics of the amplifier gain medium is studied. Effect of grating efficiency, focal spot size, pump power and other cavity parameters on the temporal behaviour of narrow band dye laser such as build-up time, pulse shape and pulse width is studied using the four level dye laser rate equation and photon evolution equation. These results are compared with experimental observations of GIG single-mode dye laser cavity. The effect of pulse stretching of CVL pump pulse on the temporal dynamics of the dye laser is studied.

Keywords. Dye laser; single longitudinal mode; rate equation.

PACS Nos 42.55.Mv; 42.60.By; 42.60.Da

1. Introduction

High-power, pulsed, single-mode, tunable dye lasers find applications in precision nonlinear laser spectroscopy of atoms and molecules, resonance ionization spectroscopy and LIDAR [1,2]. In general, a short compact laser cavity is used for obtaining single longitudinal mode laser operation with intracavity wavelength dispersion elements in the cavity for spectral discrimination of neighbouring oscillating modes. Various configurations have been reported in literature to obtain single longitudinal mode operation in pulsed dye lasers [3–9] such as direct pulsed amplification of cw dye laser, Hänsch-type cavity with intracavity etalons and short Littman-type grazing incidence grating (GIG) cavity. Among these cavities, Littman-type GIG compact cavity is a simple one which utilizes grating as the only frequency selecting component for single-mode operation without any additional beam expander and etalons. Recently, there is renewed interest in high repetition rate single-mode dye lasers pumped by copper vapour lasers (CVL) [10–15]. High repetition rate single-mode dye lasers in the visible spectrum are the only coherent source,

which are yet to be replaced with other solid-state gain media and optical parametric oscillators. The reported publications [6–15] on the single-mode GIG dye laser operating with low and high repetition rates, mainly focus on the single-mode operation and the performance characteristics of single-mode dye laser. Since single-mode dye lasers operate in a high loss cavity, a detailed theoretical study and optimization of cavity parameters are required. To the best of our knowledge, detailed theoretical studies on the temporal evolution of laser with varying cavity parameters have not been reported earlier on the single-mode dye laser. This paper reports detailed numerical study of temporal dynamics of cavity photon evolution in GIG SLM dye laser and compares theoretical results with experimental observations using pulsed GIG single-mode dye laser. Pulse widths of single-mode GIG dye lasers are observed to be shorter compared to pulse widths of the pump laser. We have carried out experimental and theoretical study of pulse stretching of single-mode GIG dye laser and presented in this paper. Pump pulse shape and the excited state transient populations are interrelated and the rate of change of excited state population dynamics closely affects both spectral and temporal behaviour of the dye laser. The frequency chirp of the dye laser during the evolution due to pulsation of population is studied for our cavity and the results are presented.

2. Experimental method

Figure 1 shows the schematic of the single longitudinal mode (SLM) dye laser cavity developed in our lab [10–12,15] based on the design of Shoshan *et al* [6] and Littman [7]. The cavity consists of a flow-through dye cell of 1 mm channel width, an end mirror ($R \sim 99\%$), tuning mirror ($R \sim 99.5\%$) and a holographic grating (2400 lines/mm) positioned at grazing angle of incidence ($\sim 89°$). The dye laser was computer-controlled for automated wavelength scanning and wavelength locking with the help of two PZTs attached to the tuning mirror and end mirror. The gain medium was Rhodamine 6G dye dissolved in ethanol. Spatially filtered green wavelength of the CVL beam ($\lambda = 510.6$ nm, beam divergence $= 0.7$ mrad) was focussed onto the dye gain medium using a plano-convex lens of 200 mm focal length. The dye cell was positioned beyond the focal

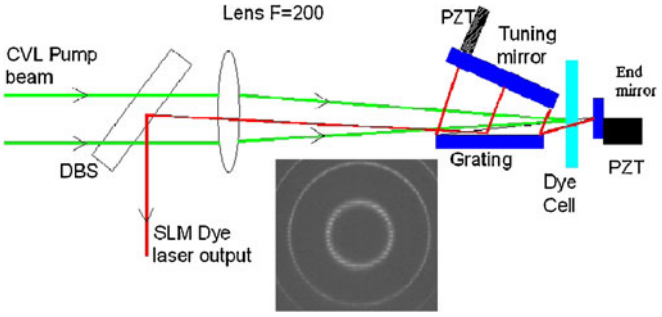

Figure 1. Schematic of SLM dye laser. Typical Fabry–Perrot spectrum of single-mode dye laser is shown in the inset. FSR of FP etalon is 7.5 GHz.

plane to prevent the damage of the end mirror. Wavelength dispersion was achieved by a holographic grating from M/s Spectrogen (2400 lines/mm, 62.5 mm length) positioned at an angle of incidence of $\sim 89^{\circ}$. The compact SLM dye laser had a cavity length of 60 mm corresponding to a cavity mode spacing of 2.5 GHz. The spectral output was measured using Fabry–Perot etalon with free spectral range of 7.5 GHz and finesse of 30 respectively. Inset of figure 1 shows the typical Fabry–Perot spectrum of the SLM dye laser.

In GIG single-mode dye laser, the pulse width reported in literature varies from 1/5th to 1/8th of the pump pulse [16,17]. This reduction of the pulse width of the dye laser indicates the high loss nature of the GIG cavity. Diffraction efficiency of the grating is generally low at 89° angle of incidence (AOI). The diffraction efficiency of grating (R_{G}) at 89° AOI measured in our lab using He–Ne laser light was 2–3%. Since the intracavity beam intersected the grating twice in one round trip, the losses in the cavity further increased. In order to optimize dye laser cavity to obtain higher peak power, longer pulse width and minimum build-up time, we have carried out numerical studies and compared the results with experiments. Temporal evolution of cavity photon number (ϕ) was studied as a function of cavity parameters such as pump beam spot size, grating efficiency, pump power and wavelength of the dye laser. In addition, the effect of temporal stretching of the pump laser pulse on the dye laser pulse was studied.

3. Theory

Modelling of SLM dye laser photon evolution in a GIG short cavity was carried out using four-level rate equation and cavity photon evolution equation [18–22]. Dye laser rate equation presented in the paper incorporates the excited state absorption from n_1 through effective stimulated emission cross-section $\sigma_{\mathrm{eff}} = \sigma_{\mathrm{e}} - \sigma_{12}$. The SLM GIG cavity was considered as a two-mirror cavity formed by an end mirror and grating–tuning mirror pair. The rate equations for the evolution of the excited state number density and cavity photon can be written as

$$\frac{\mathrm{d}n_1}{\mathrm{d}t} = \sigma_{01}(n - n_1)I - B\phi n_1 - \frac{n_1}{\tau}, \tag{1}$$

$$\frac{\mathrm{d}\phi}{\mathrm{d}t} = V_{\mathrm{g}}B\phi n_1 - \frac{\phi}{\tau_{\mathrm{c}}} + \frac{n_1 E(\lambda)g}{\tau}. \tag{2}$$

n and n_1 are the total number density and excited state number density of the dye molecules. τ and τ_{c} are the lifetime of the first excited state S1 of the dye molecule and cavity decay time respectively. σ_{01} and V_{g} are the ground state absorption cross-section of Rhodamine 6G at pump beam wavelength and gain volume of the dye medium respectively.

Dye laser was longitudinally pumped and the modelling of the pump beam intensity I incorporates the saturated pump beam absorption followed by spatial averaging over 1 mm gain length. When the peak intensity flux (photons/cm^2/s) of the pump laser beam is greater than saturation intensity, Beer–Lambert's law of exponential decay will not be

obeyed and due to high value of saturation, transmission of laser will be higher. Space averaging over the gain length with Beer's law can be written as

$$\langle I \rangle_{\text{spatial}} = \frac{\left(1 - \mathrm{e}^{-\sigma_{01} nl}\right)}{\sigma_{01} nl} I_0. \tag{3}$$

If we define saturation parameter $S = \sigma_{01} \tau_s I_p$, for GIG dye laser described in this paper, pump beam intensity at the entrance of the dye cell is higher and the corresponding saturation parameter $S > 5$. For 1 W CVL pump laser beam (6 kHz, 21 ns) focussed onto 180 micron spot radius will lead to $S = 13$. For such a large value of S, we cannot use exponential decay-based transmission. Transmission of the pump laser under saturated domain can be written as

$$\frac{\mathrm{d}I}{\mathrm{d}z} = -\frac{\sigma_{01} n I}{(1 + S)} \tag{4}$$

$$\log(T) + S(T - 1) = -\sigma_{01} nl. \tag{5}$$

Space average of the pump laser was incorporated in the programme based on the saturation-based transmission model. Transmission of the pump laser beam is given as T in eq. (5). Equation (5) was obtained by integrating absorption eq. (4) with saturation parameter over the gain length. As S increases, transmission follows almost a straight line compared to exponential decay for weaker intensities. By knowing the saturation parameter at the entrance of the dye cell, transmission of laser light intensity can be estimated from transcendental eq. (5) and spatial average can be evaluated.

B ($B = c\sigma_{\text{eff}}/V_c$) is the stimulated emission rate per photon per mode, where V_c is the volume of the cavity mode and c is the velocity of light. ϕ is the cavity photon number. Lifetime (τ) and the effective stimulated emission cross-section (σ_{eff}) at the peak wavelength of SLM dye laser used in this calculation are 5.3 ns and 1.6×10^{-16} cm^2 respectively [23]. $E(\lambda)$ and g are respectively the normalized fluorescence line shape function and geometrical factors which determine the fraction of spontaneous emission feedback into the gain medium to initiate the lasing action.

$$\tau_c = \frac{l}{c\gamma} \tag{6}$$

$$\gamma = \gamma_d + \frac{\gamma_1 + \gamma_2}{2} \tag{7}$$

$$\gamma_i = -\log[R_i] \tag{8}$$

$$\gamma_d = -\log\left(\left(1 + \left(\frac{l}{z_0}\right)^2\right)^{-1}\right). \tag{9}$$

Cavity decay time depends on the logarithmic losses including reflection, diffraction and internal losses. The parameter l in eq. (6) corresponds to the length of the cavity. Cavity decay time was calculated using logarithmic losses in the cavity. γ is the logarithmic loss factor corresponding to various feedback factors such as reflectivities (γ_1 and γ_2) and diffractional feedback (γ_d). R_1 is the reflectivity of the end mirror and R_2 is the reflectivity

Table 1. Parameters used in the calculation.

Dye laser wavelength	560 nm
Absorption cross-section σ_{01}	1.66×10^{-16} cm^2
Excited state lifetime τ [14]	5.3 ns
Stimulated emission cross-section σ_e [14]	1.6×10^{-16} cm^2
Dye concentration	0.5 mM Rhodamine 6G
Diffractional feedback for 140 micron spot diameter	79.4%
Cavity decay time	5.7×10^{-11} s

of the grating tuning mirror pair. As the GIG dye laser is a plane–plane cavity, the gain region formed by the focal spot of the pump beam is completely filled by the cavity mode of the dye laser. Diffractional feedback can be calculated in two ways: either by geometric analysis [24] or by the propagation of Gaussian beam. The parameter z_0 is the Rayleigh parameter of the focal spot radius of the pump beam which acts as the limiting aperture in the plane–plane cavity. As the end mirror was kept very close to the dye cell, diffractional losses due to the feedback from end mirror were negligible compared to the diffractional losses due to grating feedback (γ_{d}).

The cavity parameters used in the numerical analysis are: cavity length ($l = 5.6$ cm), gain medium length (=1 mm), reflectivities of the end mirror and tuning mirror ($R =$ 99%). Concentration of the dye solution chosen for the study was 0.5 mM. Table 1 shows the laser parameters used in the calculation. Cavity decay time evaluated for GIG cavity is 0.057 ns and an order less than the round trip time is 0.37 ns. Due to the small cavity decay time, GIG laser cavity is expected to be sensitive to the variation of cavity parameters.

4. Results and discussion

From rate eqs (1) and (2), the temporal evolution of the excited state population and the dye laser photon evolution inside the cavity can be evaluated. Transient population dynamics in the gain medium leads to spectral shift of the dye laser beam as it passes through the gain medium by eq. (10) [7,25].

$$\Delta\nu_l = \frac{-1}{2\lambda_l} \frac{\alpha_{\mathrm{ex}}(\nu_l)}{n_{\mathrm{s}}} \frac{\mathrm{d}}{\mathrm{d}t}(n\, l_{\mathrm{g}}). \tag{10}$$

Here the shift in the central frequency of the narrow band signal as it passes through the gain medium is given, where α_{ex} corresponds to the real part of the effective polarizability of the excited dye molecule. For Rhodamine 6G and Rhodamine B, the value was calculated to be -2×10^{-21} cm^3. In eq. (10) ground state population and the corresponding part of the effective polarizability are neglected as the low value of ground state population and along with low value of absorption cross-section at dye laser wavelength [10,25]. The parameter n_{s} corresponds to the refractive index of the solvent (in our case ethanol). By studying the population pulsation, one can estimate the spectral shift and chirping of the narrow band signal as it propagates through the gain medium. Figure 2 shows the plot of the excited state population, dye laser and the frequency shift of the dye

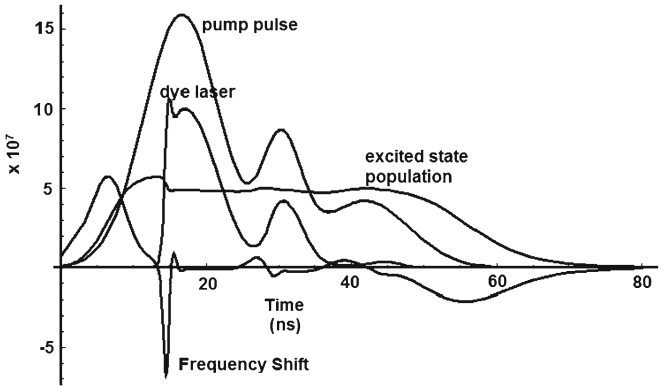

Figure 2. Plot of excited state population, dye laser and the corresponding frequency shift.

laser which depends on the population pulsation given by eq. (10). The power of the CVL laser pump, focal spot size and grating efficiency assumed for the simulation are 0.75 W, 140 μm and 2.5% respectively. In figure 2 the excited state populations, pump intensity and laser photon are shown in a reduced scale by the factor of 5×10^9, 1.2×10^{17} and 5×10^3 respectively, whereas frequency shift is shown without any reduction of the value. Four different parameters are plotted together to identify temporal details of each event, such as evolution of dye laser photon and the corresponding change in population and spectral shift dynamics.

Excited state population reaches a maximum value during the rise time of the pump pulse, followed by a small decrease in the value to reach a steady state, followed by decay after the end of the pump pulse. As the excited state population density starts to decrease from its peak value, dye laser photon begins to grow and nearly follows the pump pulse after a time delay which corresponds to the build-up time of the dye laser pulse. Frequency shift in Hz during the evolution of dye laser pulse shown in the figure corresponds to the frequency shift seen by dye laser pulse. As the dye laser pulse starts to increase from zero, spectral shift sharply grows in the negative (red-shift compared to the central frequency of the dye laser) to a minimum value of 70 MHz. A maximum effective frequency shift of 60 MHz during the evolution of dye laser photon is observed. Population pulsations lead to gain variation which in turn affects the phase temporal dynamics of the dye laser pulse passing through the gain medium.

This will introduce a spectral jitter for dye laser pulse as it evolves. FWHM of the dye laser pulse in figure 2 corresponds to 8 ns and the corresponding Fourier limit of minimum frequency width of 55 MHz and spectral chirp of 60 MHz due to population dynamics will lead to an increased spectral width of 81 MHz for single pulse spectral width. This is the minimum achievable spectral width excluding other factors contributing to the spectral width such as temperature gradients set in the gain medium due to high pulse repetition frequency (PRF) of the pump laser and flow fluctuations. If the spectral shift of the dye laser pulse occurs above the single pass spectral width of the grating, dye laser pulse will not be supported by the intracavity spectral filter such as grating in GIG and shortens the pulse width. In our laser cavity single pass spectral width was calculated to be $\sim$3 GHz (FWHM).

In the SLM dye laser, the pump beam is focussed with a spherical lens ($f = 200$ mm) into the gain medium. The size of the focal spot size affects the pumping rate ($\sigma_{01} I$) through intensity and the diffractional feedback from the grating tuning mirror pair. These two factors in turn affect the temporal dynamics of the SLM dye laser. To study the effect of the focal spot size of the pump beam at the gain medium on the intensity of the dye laser pulse, the spot size was varied from 70 micron to 220 micron. Peak pump power and the first-order diffraction efficiency of grating were assumed to be 4.76 kW and 2.5% respectively. Figure 3 shows the plot of cavity photon number as a function of time for different focal spot sizes of the pump beam. The figure also shows the scaled-down pump pulse intensity (curve H) for comparison with the dye laser pulses. From figure 3 it can be seen that the peak photon number of the dye laser for 70 micron spot size is one order less (2.0×10^{10}) compared to 200 micron spot size (3.47×10^{11}). Lower peak photon number at 70 micron spot size corresponds to lower output power and lower dye laser efficiency. Low dye laser efficiency at 70 micron spot size is due to smaller diffraction feedback to gain medium from grating–tuning mirror pair. Diffractional feedback from grating–tuning mirror pair for 70 micron and 130 micron spot radii were calculated to be 19.3% and 74.1% respectively. For smaller spot radius up to 90 micron, the rise time is slower and almost the same as the pump pulse. For spot size above 90 micron, the rise time of the dye laser is faster and the corresponding efficiency is also higher. It was observed that the peak photon number saturates beyond 170 micron spot size and starts to decrease beyond 200 micron spot size. Curve F and curve G in figure 3 correspond to the spot size of 200 micron and 220 micron respectively. Beyond 200 micron spot size, the pumping rate decreases resulting in reduced peak photon number. The lower limit on the spot size is dictated by the diffractional losses in the cavity which is 70 micron.

Single transverse mode and single longitudinal mode are to be selected for stable single-mode operation of the laser. For a single transverse mode (TEM_{00}), Fresnel number ($F = a^2/\lambda L$) of the cavity should be less than one. In the definition of Fresnel number,

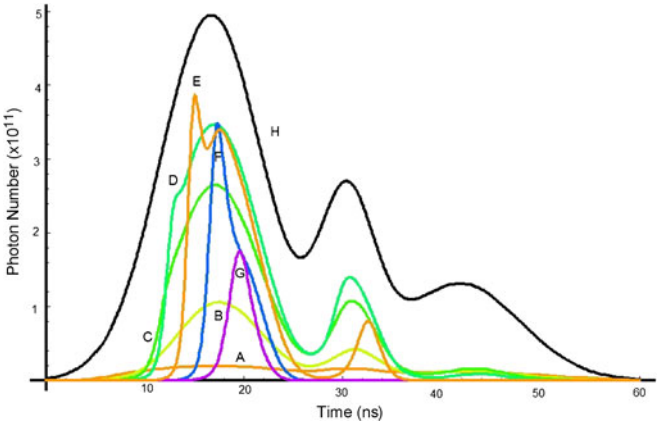

Figure 3. Effect of change in focal spot radius on dye laser cavity pulse. Spot radius assumed in the calculation for curve (A) is 70 μm, curve (B) is 90 μm, curve (C) is 110 μm, curve (D) is 130 μm, curve (E) is 170 μm, curve (F) is 200 μm and curve (G) is 220 μm. Curve (H) is the pump intensity scaled down by 10×10^{12} photons/cm^2/s.

the parameter a corresponds to the spot size and L corresponds to the length of the cavity. This limits the spot radius at the gain medium to be less than 180 micron. Therefore, the upper limit on the spot size is 180 micron. From the above discussion, we observe that in order to obtain single longitudinal mode and single transverse mode operations with longer pulse width and high efficiency, the optimum spot size for GIG SLM cavity should be between 110 micron and 150 micron.

Effect of grating efficiency on the dye laser pulse was evaluated and the results are plotted in figure 4. Grating efficiencies were varied from 2% to 10% in steps of 1%. Peak power of the pump and radius of the focal spot at the gain medium were assumed to be 5.95 kW and 140 μm respectively. Figure 4 shows the plot of pulse width and build-up time as a function of grating efficiency. Build-up time corresponds to the time delay between the start of the pump pulse and the start of the dye laser pulse. Build-up time was observed to decrease from 14.6 ns to 9 ns for a variation of grating efficiency from 2% to 10% and the pulse width changes from 5.9 ns to 11.9 ns. Build-up time decreases sharply from 14.6 ns to 10.5 ns for a variation in grating efficiency from 2% to 5% and beyond 5% grating efficiency, the reduction of build-up time and increase of pulse width are smaller. The reflective feedback of grating–tuning mirror pair (R_2) for the grating efficiency of 5.5% is 4.6 times more compared to feedback for a grating efficiency of 2.5% because the grating is seen twice in one round trip and the effective reflectivity depends quadratically on the value of the grating efficiency. Though the reduction of laser build-up time with increase in grating efficiency is known, the sensitivity of grating efficiency on dye laser dynamics of GIG single-mode cavity is observed to be high. The optical delay requirement for the synchronization of SLM oscillator signal and the amplifier gain in the dye amplifier is critically dependant on the SLM dye laser build-up time. Minimum

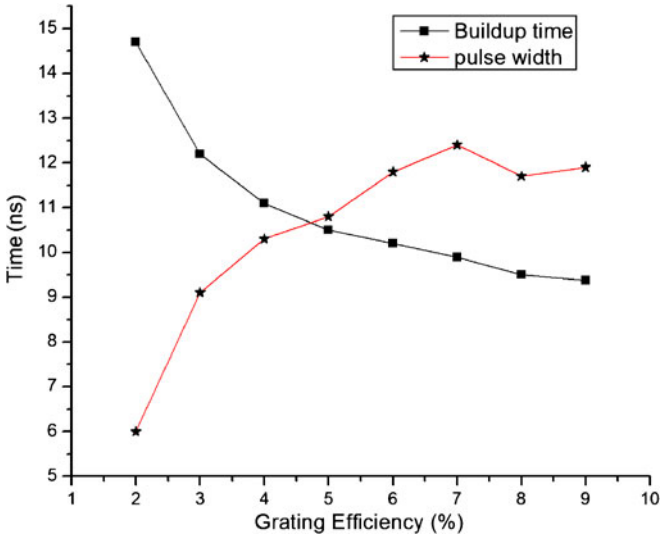

Figure 4. Effect of change in grating diffraction efficiency on the dye laser pulse width and build-up time.

build-up time of SLM dye oscillator along with longer pulse width is desirable for the amplification of SLM dye signal in the successive amplifier stages.

Figure 5 shows the effect of pumping rate on the single-mode dye laser pulse. The parameters assumed for this calculation were 2.5% grating efficiency and 140 micron focal spot size. Theoretical results are shown as solid line and dashed line whereas the experimental data are shown as points. When pumping rates ($\sigma_{01} I$) were varied from 3×10^9 s^{-1} to 7.6×10^9 s^{-1}, the corresponding build-up time decreased from 15 ns to 12 ns. Pulse width was observed to increase from 4.8 ns corresponding to a low pump rate of 3×10^9 s^{-1} to 9.85 ns corresponding to a higher pump rate of 7.6×10^9 s^1. At lower pump rate, the rise time of the dye laser pulse was observed to be longer compared to the rise time of the dye laser pulse at higher pump rates. At higher pump rates, the dye laser temporal pulse follows the copper vapour laser pulse with a time lag.

The evolution of the dye laser pulse at different wavelengths of operation was studied. CVL pump peak power of 5.95 kW, spot radius of 140 micron and grating efficiency of 2.5% were assumed. In our lab, the single-mode dye laser operated with a tuning range of 12 nm with a peak wavelength at 560 nm for Rhodamine 6G gain medium [10, 11]. The effective stimulated emission cross-section peaked at 560 nm and decreased symmetrically on both sides of the peak wavelength [23]. At the peak of the tuning range, the dye laser build-up time was observed to be 12 ns and at the end of the tuning range the build-up time increased to 17 ns. Pulse width was observed to reduce from 7.5 ns to 4 ns from the peak to the end of the tuning range of the dye laser. The effective stimulated emission cross-section was higher at the peak of the tuning range and the available population inversion of the dye molecules was effectively extracted into the dye laser photons whereas at the wings of the tuning range the effective stimulated emission cross-section was lower.

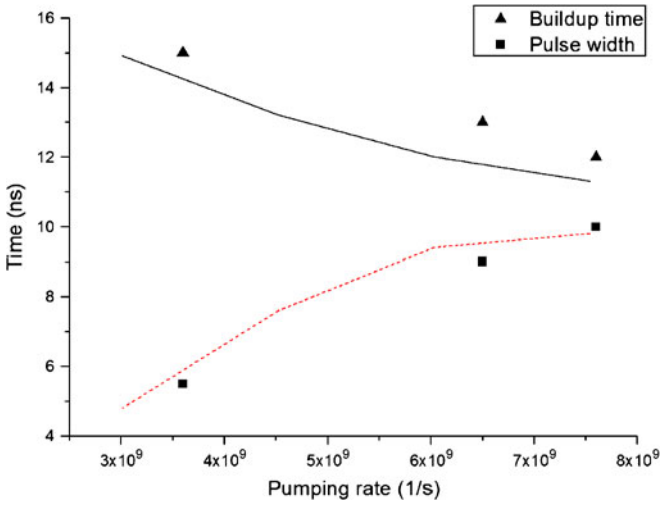

Figure 5. Effect of pump power variation on the dye laser build-up time and pulse width. Experimental data are marked as triangular and square symbols. Theoretical data are shown as solid line and dashed line.

Minimum build-up time, maximum pulse width and maximum dye laser efficiency are obtained with optimized cavity parameters such as spot size (∼140 micron), high grating efficiency (>5%) and wavelength of operation. Pumping rate should be higher for longer pulse width and higher efficiency of the dye laser but restricted to a value lower than a value which excites the second mode to oscillate due to spatial-hole burning of the standing wave cavity. In figure 4 we have assumed values for pumping rate for single-mode operation regime as observed in our experiments.

In the SLM dye laser pulse duration was experimentally observed to be shorter (∼6 ns) compared to CVL pump pulse. To achieve higher efficiency and lower amplified spontaneous emission in the dye amplifiers, the pulse width of the SLM dye laser should be as close to pump pulse as possible. One technique for obtaining longer pulse duration of the dye laser is by temporal stretching of the pump laser beam. We have carried out experimental and theoretical studies on the temporal pulse stretching of the SLM dye laser. The SLM dye laser was pumped with temporally stretched CVL laser pulse using a compact triangular passive ring cavity as the pulse stretcher [26] which utilizes beam splitter (30/70; R/T). The stretcher arrangement is shown in the inset of figure 6. When the stop (S) was introduced in the stretcher arm, the dye laser was pumped with unstretched pump pulse and the dye laser was pumped by stretched pulse as the stop was removed. The pump pulse after the stretcher will have spatial overlap of unstretched part (30% of I) and different stretched components with successive delays and reduced power. One more advantage of pulse stretching is that the shape of the pump pulse will be smooth compared to CVL pulse from unstable resonator. This will result in a minimum variation of rate of change of the excited state population and results in reduced spectral shift of the dye laser in the cavity photon evolution period.

$$I_{\mathrm{st}}(t) = I\left(RI(t) + (1-R)^2 \sum_{n=1}^{\infty} R_1^n R_2^n R^{n-1} I\,(t - n\tau_{\mathrm{r}})\right). \tag{11}$$

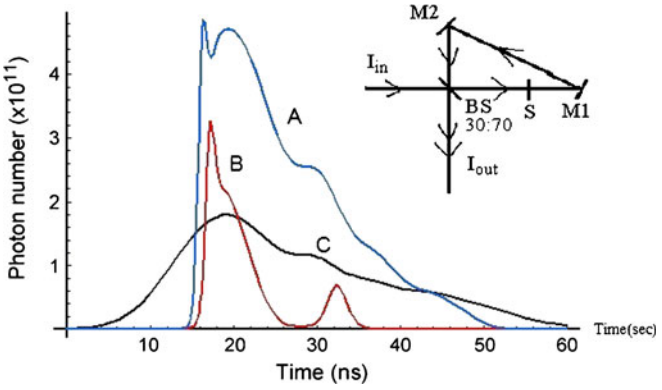

Figure 6. Effect of pulse stretching of the CVL pulse on the dye laser output. Curve A corresponds to stretched pump beam intensity (scaled down by 1×10^{14} photons/cm^2/s), curve B corresponds to unstretched dye laser output and curve C corresponds to dye laser output pumped with stretched pump pulse.

Pump laser pulse was modelled as per eq. (11) to study the effect of stretched pump pulse on dye laser output. The parameter I_{st} is the output pump beam from the stretcher, I is the input pump beam intensity to stretcher, R is the reflectivity of the beam splitter, R_1 and R_2 are the reflectivities of the mirrors M1 and M2, τ_r is the passive delay of the ring cavity. For the dye laser under study, only two components of the ring cavity output, namely first stretched component (49% of I) and the second successive component (14.7% of I) will affect the laser dynamics. These two components are included in the modelling of stretched pump pulse as per eq. (11) and the results of the dye laser evolution are plotted in figure 6.

The reflectivities of the cavity mirrors (R_1 and R_2) of the pulse stretcher were assumed to be closer to unity. The optical delay of the stretcher arm was chosen as 5.7 ns and the input peak power (I) before the pulse stretcher of 20 kW was assumed in the calculation. Rise time of both stretched dye laser pulse and the unstretched pulse remained the same and build-up time slightly reduced for the stretched dye laser pulse. Pulse width of the unstretched and stretched dye laser pulse was 4.5 ns and 15.3 ns. Stretching of the dye laser pulse is due to the longer pulse width of the pump beam and also the additional power in the stretched part of the pump beam. The pulse shape and extent of stretching of laser pulse depend on the time delay of the ring cavity and input pump peak power.

5. Experimental observation

The effect of grating efficiency on build-up time and pulse width of the SLM dye laser was experimentally studied. Figure 7 shows the oscilloscope trace of the CVL pump pulse and dye laser pulse for low pump rate (3.6×10^9 s^{-1}). The grating used in the laser cavity had a grating efficiency of 2–3% at 89° angle of incidence. The pulse width of the pump

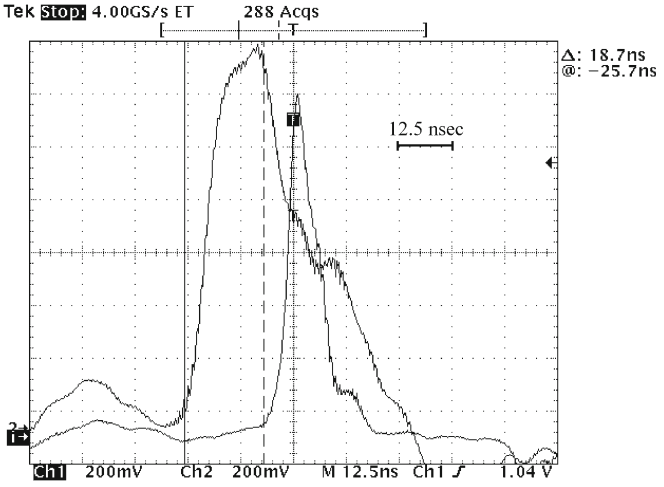

Figure 7. Oscilloscope trace of CVL pump pulse and SLM dye laser pulse for low efficiency grating.

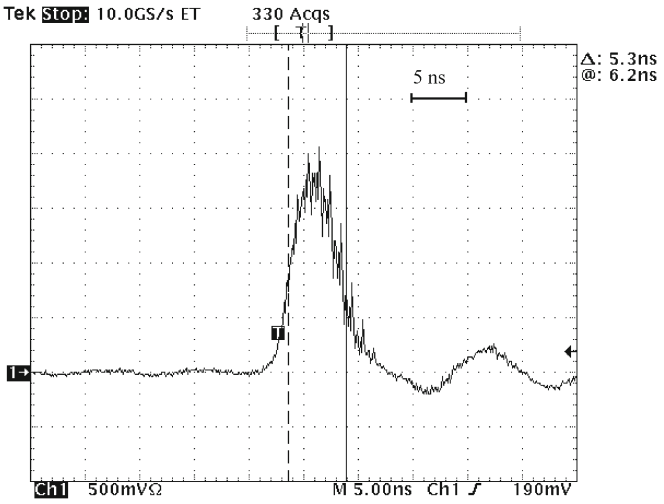

Figure 8. Unstretched SLM dye laser pulse.

pulse used in this experiment was 21 ns. The pulse width of the dye laser was 5–6 ns. The single-mode dye laser pulse width was approximately 1/4th of the pulse width of pump laser. From figure 7, the dye laser build-up time was measured to be 15.7 ns after correcting passive delay of 3 ns.

A high-efficiency GIG grating from M/s Optometrics Corporation was utilized in SLM dye laser. Theoretical efficiency of these gratings at 89° is above 12% at 560 nm. The efficiency of the grating was experimentally measured to be 6–8% at 89° angle of incidence. The pump laser pulse width was 24 ns and dye laser pulse width was measured to be 10 ns. The build-up time between the CVL and dye laser with high efficiency grating

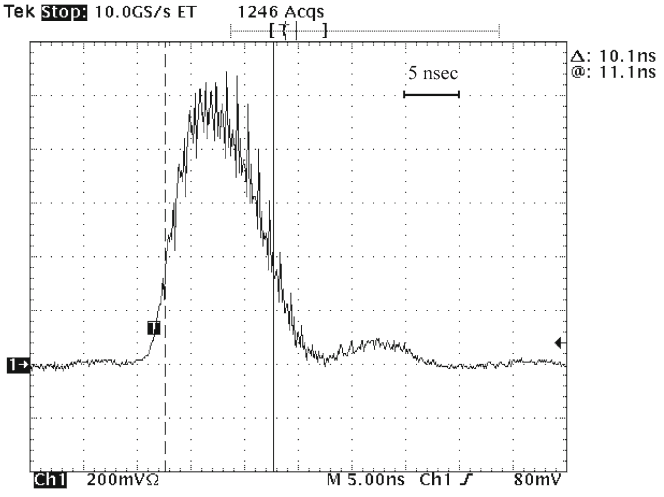

Figure 9. Stretched SLM dye laser pulse.

was observed to be 7 to 8 ns compared to 12 ns with low-efficiency grating at similar pump rates [11]. New designs of grating with high efficiency at grazing angle of incidence (∼89°) are reported in [27]. Major loss in the GIG single-mode dye laser is due to grating efficiency and the improved efficiency of the GIG grating will make this cavity an ideal cavity for single-mode operation.

Effect of pulse stretching of the pump laser pulse on the SLM dye laser was experimentally studied. Pulse stretching of the pump laser was done with compact triangular pulse stretcher as shown in figure 6. A peak power of 20 kW was fed to the pulse stretcher. With ring cavity length corresponding to the cavity round trip time of 5.7 ns, CVL pulse was stretched from 15 ns to smooth 28 ns pulse. Figure 8 shows the unstretched dye laser pulse and figure 9 shows the dye laser pulse pumped by stretched CVL laser pulse. The dye laser pulse was stretched from 5.3 ns to 10 ns (66% of the unstretched pump laser pulse width). Theoretical results predict the stretching of dye laser pulse to 15 ns (71% of the unstretched pump laser width) under similar parameters of pulse stretcher. Unstretched pump laser pulse width assumed in the theory was 21 ns. The shape of the dye laser pulse and pulse width were experimentally observed to vary as a function of passive ring cavity round trip time. The shape of the dye laser output pulse was observed to change from single peak pulse to double peak pulse with the delay of the stretcher arm from 5 ns 11 ns. By using the pulse stretcher, the shape of the CVL pump pulse can be altered to smooth pulse shape which in turn generates smooth dye laser pulse with longer pulse duration. Smoother pump pulse shape is expected to give minimum population pulsation which in turn affects both spectral and temporal evolution of SLM dye laser.

6. Conclusion

We have presented the experimental and theoretical study of narrow-band dye laser photon evolution in pulsed single-mode dye laser cavity. Modelling of SLM photon evolution using four-level rate equations in a GIG short cavity is presented. Due to small cavity decay time (0.057 ns), temporal dynamics was observed to be very sensitive to the variation of cavity parameters. Effective frequency chirp of the single-mode dye laser during the evolution due to transient population dynamics was estimated. From the simulation, the optimum cavity parameters such as spot size, grating efficiency and the pump rate for high conversion efficiency and longer pulse width of the single-mode dye laser were estimated. The optimum spot size at the dye cell for single-mode operation with higher pulse width and efficiency were found to be in the range of 110 to 150 micron. Build-up time was observed to reduce by 30% and the pulse width was increased by 80% for a change in grating efficiency from 2% to 5%. Dye laser pulse was temporally stretched experimentally from 5.3 ns to 10 ns using three-mirror compact pump beam pulse stretcher. Theoretical results predict the pulse stretching of dye laser to be 71% of the unstretched pump pulse which matched closely with experimental observation. Using the pulse stretching of the pump beam, the pulse width and pulse shape of the single-mode dye laser pulse can be controlled. GIG single-mode dye laser cavity with optimized cavity parameters such as grating efficiency, focal spot diameter and pump power will make this cavity an ideal candidate for pulsed single-mode operation.

References

[1] R V Ambartzumian and V S Letokhov, *Appl. Opt.* **11**, 354 (1972)
[2] E A Hildum, U Boesl, D H McIntyre, R G Beausoleil and T W Hansch, *Phys. Rev. Lett.* **56**, 576 (1986)
[3] T W Hansch, *Appl. Opt.* **11**, 895 (1972)
[4] A F Bernhardt and P Rasmussen, *Appl. Phys. B* **26**, 141 (1981)
[5] Yoichiro Maruyama, Masaaki Kato, Akira Sugiama and Takashi Arisawa, *Opt. Commun.* **81**, 67 (1991)
[6] I Shoshan, N N Danon and U P Oppenheim, *J. Appl. Phys.* **48**, 4495 (1977)
[7] M G Littman, *Opt. Lett.* **3**, 138 (1978)
[8] I T Mckinnie, A J Berry and T A King, *J. Mod. Opt.* **38**, 1691 (1991)
[9] S A Kostritsa and V A Mishin, *Quant. Electron.* **25**, 1687 (1992)
[10] G Sridhar, V S Rawat, S Singh and L M Gantayet, accepted for publication in *J. Opt.* (2013), DOI: 10.1007/s12596-012-0099-4
[11] V S Rawat, G Sridhar, S Singh and L M Gantayet, accepted for publication in *Optik Journal*
[12] V S Rawat, G Sridhar, N Kawade, S Singh and L M Gantayet, *Laser Phys.* **23**, 035002 (2013)
[13] O Prakash, J Kumar, R Mahakud, P Saxena, V K Dubey, S K Dixit and J K Mittal, *Opt. Laser Technol.* **43**, 1475 (2011)
[14] O Prakash, R Mahakud, P Saxena, V K Dubey, S K Dixit and J K Mittal, *Opt. Commun.* **283**, 5099 (2010)
[15] G Sridhar, V S Rawat, Nitin Kawade, Sunita Singh and L M Gantayet, *Pramana – J. Phys.* **75**, 807 (2010)
[16] Jonghoon Yi, Jin-Tae Kim, Hee-Jong Moon, Sipyo Rho, Jaemin Han, Yongjoo Rhee and Jongmin Lee, *J. Korean Phys. Soc.* **35**, 275 (1999)
[17] Yoichiro Maruyama, Masaaki Kato and Takashi Arisawa, *Jpn. J. Appl. Phys.* **30(48)**, L748 (1991)
[18] A Shevchenko *et al*, *Appl. Phys. B* **74**, 349 (2002)
[19] O Svelto, *Principles of lasers*, 5th edn (Springer, 2010)
[20] P P Sorokin, J R Lankard, E C Hammond and V L Maruuzzi, *IBM J.* **11**, 130 (1967)
[21] C Lin, *IEE J. Quant. Electron.* **11**, 602 (1975)
[22] S Jelvani and B Khodadoost, *Opt. Laser. Technol.* **39**, 182 (2007)
[23] Paul C Beaumont, David G Johnson and Bary J Parsons, *J. Chem. Soc. Faraday Trans.* **89**, 4185 (1993)
[24] L G Nair and K Dasgupta, *IEEE J. Quantum. Electron.* **21**, 1782 (1985)
[25] N Melikechi, S Gangopadyay and E E Eyler, *J. Opt. Soc. Am.* **11**, 2402 (1994)
[26] Jun Kojima and Quang-Viet Nguyen, *Appl. Opt.* **41**, 6360 (2002)
[27] S V Vasil'ev, V A Sychugov and B A Usievich, *J. Russ. Las. Res.* **21**, 561 (2000)